⌘ *Author's Choice*

THE JOURNAL OF BIOLOGICAL CHEMISTRY VOL. 285, NO. 26, pp. 20192–20201, June 25, 2010

Efficient Phagocytosis Requires Triacylglycerol Hydrolysis by Adipose Triglyceride Lipase*

Received for publication, January 26, 2010, and in revised form, April 20, 2010 Published, JBC Papers in Press, April 27, 2010, DOI 10.1074/jbc.M110.107854

Prakash G. Chandak[‡], Branislav Radović[‡], Elma Aflaki[‡], Dagmar Kolb[‡§], Marlene Buchebner[‡], Eleonore Fröhlich[¶], Christoph Magnes[‖], Frank Sinner[‖], Guenter Haemmerle[§], Rudolf Zechner[§], Ira Tabas[**], Sanja Levak-Frank[‡], and Dagmar Kratky[‡1]

*From the [‡]Institute of Molecular Biology and Biochemistry, Center of Molecular Medicine, Medical University of Graz, Harrachgasse 21, 8010 Graz, Austria, the [§]Institute of Molecular Biosciences, University of Graz, Heinrichstrasse 31/Humboldstrasse 50, 8010 Graz, Austria, the [¶]Center for Medical Research, Medical University of Graz, Stiftingtalstrasse 24, 8010 Graz, Austria, [‖]Joanneum Research, Institute of Medical Technologies and Health Management, Stiftingtalstrasse 24, 8010 Graz, Austria, and the **Departments of Medicine, Pathology and Cell Biology, and Physiology and Cellular Biophysics, Columbia University, New York, New York 10032*

Macrophage phagocytosis is an essential biological process in host defense and requires large amounts of energy. To date, glucose is believed to represent the prime substrate for ATP production in macrophages. To investigate the relative contribution of free fatty acids (FFAs) in this process, we determined the phagocytosis rates in normal mouse macrophages and macrophages of adipose triglyceride lipase (ATGL)-deficient mice. ATGL was shown to be the rate-limiting enzyme for the hydrolysis of lipid droplet-associated triacylglycerol (TG) in many tissues. Here, we demonstrate that *Atgl*$^{-/-}$ macrophages fail to efficiently hydrolyze cellular TG stores leading to decreased cellular FFA concentrations and concomitant accumulation of lipid droplets, even in the absence of exogenous lipid loading. The reduced availability of FFAs results in decreased cellular ATP concentrations and impaired phagocytosis suggesting that fatty acids must first go through a cycle of esterification and re-hydrolysis before they are available as energy substrate. Exogenously added glucose cannot fully compensate for the phagocytotic defect in *Atgl*$^{-/-}$ macrophages. Hence, phagocytosis was also decreased i*n vivo* when *Atgl*$^{-/-}$ mice were challenged with bacterial particles. These findings imply that phagocytosis in macrophages depends on the availability of FFAs and that ATGL is required for their hydrolytic release from cellular TG stores. This novel mechanism links ATGL-mediated lipolysis to macrophage function in host defense and opens the way to explore possible roles of ATGL in immune response, inflammation, and atherosclerosis.

A critical role of macrophages in host defense and resolution of inflammation is to phagocytose pathogens and cellular debris, which are then enclosed in specific vacuoles called phagosomes. Phagosomes then fuse with lysosomes, yielding phagolysosomes where enzymatic degradation occurs. Phagocytosis is a process that demands a large supply of energy, most likely to combat infections and remove debris in damaged tissues. Normally, glucose is the favored fuel to generate ATP. *In vitro*, however, macrophages also generate ATP from glutamine, lactate, keto acids, and fatty acids (FAs)[2] to varying degrees (1, 2). In this regard, Yin *et al.* (3) have shown that FAs produced by macrophage lipoprotein lipase (LPL) acting on triacylglycerol (TG)-rich lipoproteins provide an important source of energy for phagocytosis but not endocytosis. FAs in the circulation are bound to albumin or transported in esterified forms within TG-rich lipoproteins, notably VLDL. VLDL causes accumulation of TG and FAs in macrophages through uptake of FAs produced by extracellular LPL-mediated VLDL lipolysis or by endocytosis of whole VLDL particles and VLDL remnants, whose TG stores are subsequently hydrolyzed in lysosomes (4–7). Several groups have demonstrated that LPL-mediated FA generation affects atherogenesis. For example, it was found that atherosclerosis susceptibility is increased in mice with high expression levels of LPL in macrophages (8–10) and is reduced in mice that lack LPL (11).

Essentially all mammalian cells, including macrophages, generate lipid droplets as storage organelles consisting of neutral lipids (cholesteryl esters (CE) and TG), phospholipids, unesterified free cholesterol (FC), and lipid droplet-associated proteins (12–14). In the setting of atherosclerosis, macrophages have an enormous capacity to take up cholesterol-rich apolipoprotein B-containing lipoproteins by clathrin-mediated endocytosis, pinocytosis, and phagocytosis (15, 16). This process results in the accumulation of CE droplets in the cytoplasm of the cells, giving them a "foamy" appearance. Intimal macrophage foam cells are a characteristic feature of atherosclerotic lesions.

Excess intracellular accumulation of FFAs can be toxic to cells (17). Therefore, cells protect themselves from this over-

* This work was supported, in whole or in part, by National Institutes of Health Grants HL54591 and HL75662. This work was also supported by the Austrian Science Fund FWF SFB-LIPOTOX F30 and P19186, the Austrian Federal Ministry of Science and Research GEN-AU Project Genomics of Lipid-associated Disorders, and the Medical University of Graz (Ph.D. Program for Molecular Medicine).

⌘ *Author's Choice*—Final version full access.

[1] To whom correspondence should be addressed. Tel.: 43-316-380-7543; Fax: 43-316-380-9615; E-mail: dagmar.kratky@medunigraz.at.

[2] The abbreviations used are: FA, fatty acid; ATGL, adipose triglyceride lipase; TG, triacylglycerol; CE, cholesteryl esters; FC, free cholesterol; FFA, free fatty acid; LPL, lipoprotein lipase; MPM, murine peritoneal macrophages; ac, acetylated; agg, aggregated; DMEM, Dulbecco's modified Eagle's medium; PBS, phosphate-buffered saline; LPDS, lipoprotein-deficient serum; LDL, low density lipoprotein; VLDL, very LDL; WT, wild type; BMM, bone marrow-derived macrophage.

load by esterifying and thereby neutralizing excess FAs into TG and CE. The consequences of FC *versus* CE accumulation in macrophages have been thoroughly studied (18–21). In contrast, much less is known about the molecular and (patho)physiological effects of FA *versus* TG accumulation in macrophages. Both FAs and FC are released from lipid droplets by intracellular lipases. Adipose triglyceride lipase (ATGL) catalyzes the initial step of TG hydrolysis in many tissues, generating diacylglycerol and FFAs (22–25). Hormone-sensitive lipase was shown to be more important as diacylglycerol than TG hydrolase (26). The enzymatic function and physiological role of hormone-sensitive lipase in macrophages in neutral CE hydrolysis are still a matter of debate (27–30). The final step in TG hydrolysis is conducted by monoacylglycerol lipase that specifically cleaves monoacylglycerol to yield glycerol and FFA (31).

Here, we demonstrate that macrophages express considerable amounts of enzymatic active ATGL. In the absence of ATGL, macrophages accumulate high amounts of TG-rich lipid droplets. The lipolytic defect and consequently the reduced availability of FAs in $Atgl^{-/-}$ macrophages decrease the capacity for phagocytosis even in the presence of glucose.

EXPERIMENTAL PROCEDURES

Animals—Animal experiments were performed in accordance with the standards established by the Austrian Federal Ministry of Science and Research, Division of Genetic Engineering and Animal Experiments (Vienna, Austria). All experimental protocols were approved by the Ethics Committee for Animal Experiments of the Medical University of Graz, Austria. $Atgl^{-/-}$ mice (25) and WT littermates (on a C57Bl/6 background) were maintained in a clean environment on a regular light-dark cycle (12 h light, 12 h dark) on a standard laboratory chow diet containing 4% fat and 21% protein (R/M-H; Ssniff, Soest, Germany).

Cell Culture—Peritoneal macrophages were obtained 3 days after intraperitoneal injection of 3 ml of 3% thioglycollate. Macrophages were cultured in DMEM, 10% LPDS (Invitrogen) supplemented with 1% penicillin, 1% streptomycin for 2 h. Thereafter, cells were washed twice with PBS, and if not stated otherwise, the adherent macrophages were cultured in high glucose (25 mM) DMEM containing 4 mM glutamine, 1 mM pyruvate, and 10% LPDS. In some experiments, macrophages were incubated in DMEM containing 0, 6, or 25 mM glucose. LDL and VLDL were isolated from human plasma by density gradient ultracentrifugation, and LDL was acetylated as described previously (32). Protein was quantitated using the Bradford assay (Bio-Rad). For isolation of bone marrow-derived macrophages, femur and tibia were removed and flushed with 2 ml of DMEM. Bone marrow cells were plated in DMEM, 10% LPDS, 1% penicillin, 1% streptomycin and differentiated into macrophages by addition of 10 ng/ml macrophage colony-stimulating factor (R & D Systems, Minneapolis, MN) for 8 days.

Real Time PCR—Total RNA from macrophages and foam cells was isolated using RNeasy mini kit (Qiagen, Hilden, Germany). Total RNA from white and brown adipose tissues was isolated using TRIzol (Invitrogen). Two micrograms of total RNA were reverse-transcribed by using the high capacity cDNA reverse transcription kit (Applied Biosystems, Foster City, CA). Quantitative real time PCR was performed on a LightCycler 480 (Roche Diagnostics) using the Quantifast™ SYBR® Green PCR kit (Qiagen, Hilden, Germany). Primer sequences are available upon request. Amplification of human porphobilinogen deaminase and murine hypoxanthine-guanine phosphoribosyltransferase as housekeeping genes was performed on all samples as internal controls for variations in mRNA amounts.

Western Blotting Analysis—Equivalent amounts of protein homogenates were resolved by 10% SDS-PAGE, transferred to a nitrocellulose membrane, and probed with rabbit polyclonal antibodies to murine ATGL (1:200), hormone-sensitive lipase (1:800) (Cell Signaling Technology, Danvers, MA), and a monoclonal anti-mouse β-actin (1:5000) (Santa Cruz Biotechnology). Specifically bound immunoglobulins were detected in a second reaction with a horseradish peroxidase-labeled IgG conjugate and visualized by enhanced chemiluminescence detection (ECL Plus, GE Healthcare).

Assay for TG and CE Hydrolase Activity—MPM were washed two times with PBS and sonicated (Labsonic B. Braun, Melsungen, Germany) twice for 10 s in 100 mM potassium phosphate lysis buffer (250 mM sucrose, 1 mM EDTA, 1 mM dithiothreitol, 20 μg/ml leupeptin, 2 μg/ml antipain, 1 μg/ml pepstatin (pH 7.0)). Nuclei and cell debris were removed by centrifugation (1000 $\times$ *g*) for 5 min at 4 °C. Protein concentrations were quantitated using the Bradford assay (Bio-Rad). One hundred μg of protein from cell lysates were incubated in a water bath at 37 °C for 1 h with 100 μl of substrate. TG substrate contained 25 nmol of triolein/assay and 40,000 cpm/nmol [9,10-^{3}H]triolein (PerkinElmer Life Sciences) as tracer. CE substrate contained 20 nmol of cholesteryl oleate/assay and 50,000 cpm/nmol of cholesteryl [1-^{14}C]oleate (Amersham Biosciences) as tracer. All lipid substrates were prepared by sonication (Labsonic, B. Braun, Melsungen, Germany) as described previously (33). The reaction was terminated by the addition of 3.25 ml of methanol/chloroform/hexane (10:9:7, v/v) and 1 ml of 100 mM potassium carbonate, 100 mM boric acid (pH 10.5). After centrifugation (800 $\times$ *g*, 20 min), the radioactivity in 1 ml of the upper phase was determined by liquid scintillation counting, and the release of FFA was calculated.

Lipid Parameters in Macrophages—Lipids from MPM were extracted with 2 ml of hexane/isopropyl alcohol (3:2, v/v) for 1 h at 4 °C. Lipid extracts were dried under nitrogen, redissolved in 100 μl of Triton X-100 in chloroform, dried under nitrogen, and resuspended in 100 μl of distilled water for 15 min at 37 °C. Aliquots (30 μl) were used for enzymatic measurements of TG (Diagnostic Systems, Holzheim, Germany), total cholesterol (Greiner Diagnostics AG, Bahlingen, Germany), and FC (Diagnostic Systems, Holzheim, Germany) concentrations. Protein was quantitated using a Bradford assay (Bio-Rad) after dissolving the proteins of extracted cells in 2 ml of 0.3 M NaOH for 1 h at room temperature.

Electron Microscopy—MPM grown on a Melinex Film (Gröpl, Tulln, Austria) were fixed in 0.06 M phosphate buffer (pH 7.2) containing 2.5% glutaraldehyde for 90 min at room temperature. MPM were rinsed twice in 0.06 M phosphate buffer for 10 min and post-fixed in 1% osmium tetroxide in the

same buffer for 1 h. The cells were then rinsed four times for 10 min in 0.06 M phosphate buffer and dehydrated in 50, 70, 90, and 100% cold acetone for 20 min each. Thereafter, cells were infiltrated by 2:1, 1:1, and 1:2 mixtures of 100% acetone and agar 100 epoxy resin (Gröpl, Tulln, Austria) and pure agar 100 epoxy resin for 4 h. The cells were then placed in agar 100 epoxy resin at room temperature for 8 h, transferred into embedding molds, and polymerized at 60 °C for 48 h. Ultrathin sections (75 nm) were cut with a Reichert Ultracut S ultramicrotome and stained with lead citrate for 5 min and with uranyl acetate for 15 min. Images were taken on a Philips CM 10 transmission electron microscope equipped with a plate camera system.

Nile Red Staining and Fluorescence Microscopy—MPM from WT and *Atgl*$^{-/-}$ mice were plated on chamber slides in DMEM, 10% LPDS for 24 h. Cells were fixed with 4% paraformaldehyde for 30 min, and lipid droplets were visualized after Nile Red staining (2.5 μg/ml) by confocal laser scanning microscopy using an LSM 510 META microscope system (Carl Zeiss GmbH, Vienna, Austria). Pictures (×63) were taken at excitation 543 nm, and signals were recorded using a 560-nm long pass filter. Quantification of lipid droplet-containing cells in MPM and foam cells was performed in at least 150 cells per group using Zeiss LSM Image Browser (Carl Zeiss Microimaging GmbH, Vienna, Austria).

acLDL and VLDL Labeling with [^{3}H]Cholesterol or [9,10-^{3}H]Triolein—One hundred μg of freshly prepared acLDL/ml were enriched with 1 μCi of [1,2-^{3}H]cholesterol (Hartmann Analytik, Braunschweig, Germany). One hundred μg of VLDL/ml were enriched with 1 μCi of [9,10-^{3}H]triolein (GE Healthcare). The mixtures were overlaid with argon and incubated for 16 h at 37 °C under continuous shaking. Labeled lipoproteins were separated from unincorporated [^{3}H]cholesterol or [9,10-^{3}H]triolein and desalted by exclusion chromatography on PD-10 columns (Amersham Biosciences) using PBS as eluent.

Lipoprotein and Oleate Uptake—MPM of *Atgl*$^{-/-}$ and WT mice were plated in 12-well plates and incubated with 1 μCi of [^{3}H]acLDL and [^{3}H]VLDL at 37 °C for 24 h, respectively. After incubation, cells were washed with PBS and lysed in 1 ml of 0.3 M NaOH, and the incorporated radioactivity was determined by scintillation counting. Protein content was quantitated using the Bradford assay (Bio-Rad).

For determination of oleate uptake and incorporation of oleate into lipid subclasses, MPM of *Atgl*$^{-/-}$ and WT mice were plated in 12-well plates and incubated with 1 μCi of [^{3}H]oleate (GE Healthcare) and 200 μM oleate in DMEM containing 1% FFA-free bovine serum albumin for 6 h at 37 °C. Thereafter, cells were washed twice with PBS and dried, and the lipids were extracted with 1 ml of hexane/isopropyl alcohol (3:2, v/v) on a rotary shaker for 1 h at 4 °C. Five-μl aliquots were assayed for oleate uptake by scintillation counting. Lipids were dried under a stream of nitrogen, redissolved in 100 μl of human serum/chloroform/methanol (1:1:1, v/v) and separated by thin layer chromatography (hexane/diethyl ether/acetic acid, 65:35:1). The bands were excised, and the incorporation of [^{3}H]oleate into various lipid subclasses was quantitated by scintillation counting.

LPL Assay—MPM were incubated in 12 wells with 1 ml of medium, 2% FFA-free bovine serum albumin (Sigma), and 2 units of heparin for 1 h at 37 °C. For the substrate preparation per sample, 0.6 μCi of [^{3}H]triolein, 920 ng of nonradioactive glycerol trioleate, and 0.1% Triton X-100 in chloroform were evaporated under a stream of nitrogen. Forty μl of 1 M Tris-HCl (pH 8.6) and 80 μl of double distilled H_2O were added, and the mixture was sonicated six times (1 min on and 1 min off) on ice. Then 40 μl of heat-inactivated human serum containing apoCII as activator (obtained from a pool of donors, heated at 50 °C for 1 h and stored at −20 °C) and 40 μl of 10% FFA-free bovine serum albumin were added to the substrate. For the analysis, 200 μl of the substrate were incubated with 100 μl of the sample for 1 h at 37 °C. The reaction was stopped by the addition of 3.25 ml of a mixture of methanol/chloroform/heptane (1.41:1.25:1, v/v) and 1 ml of 100 mM potassium carbonate and 100 mM boric acid (pH 10.5). FFA were extracted by vortex mixing for 10 s, and phases were separated by centrifugation at 3200 rpm for 10 min. Radioactivity in 1 ml of the upper phase was measured by liquid scintillation counting. MPM were lysed, and protein was quantitated by the method of Bradford.

Analysis of ATP Concentrations and ADP/ATP Ratios—Intracellular ATP levels of *Atgl*$^{-/-}$ and WT MPM were measured in DMEM containing 0, 6, or 25 mM glucose using EnzyLight™ ATP assay (BioAssay Systems, Hayward, CA) according to the manufacturer's instructions. Oligomycin (0.5 μM), an inhibitor of F_1F_0-ATP synthase, was used as an ATP depletion control (34, 35). Luminescence was measured on a TopCount NXT luminometer (Packard Instruments, Meriden, CT) and quantitated to ATP standards. ADP/ATP ratios were determined using EnzyLight™ ADP/ATP ratio assay kit (BioAssay Systems).

Acyl-CoAs and Carnitine Esters—Acyl-CoAs were determined by on-line solid phase extraction liquid chromatography-mass spectrometry as described previously (36). This method also allowed the separation and semiquantitative analysis of acylcarnitines. Acyl-CoAs (internal standards of 0.5 nmol/ml C17:0 CoA, 0.6 nmol/ml $^{13}C_2$-acetyl-CoA, and 0.6 nmol/ml $^{13}C_3$-malonyl-CoA) and acylcarnitines (internal standard of 0.5 nmol/ml C17–0 CoA) were extracted from the cell pellet using 0.5 ml of prechilled (4 °C) buffer (50% 0.1 M KH_2PO_4 and 50% 2-propanol). The cell suspension was homogenized on ice for 10–20 s using an ultrasonic homogenizer. Subsequently, 30 μl of saturated aqueous $(NH_4)_2SO_4$ and 0.5 ml of acetonitrile were added. The homogenate was vigorously mixed and centrifuged at 2,500 × *g* for 10 min at 4 °C, and the supernatant was transferred to autosampler vials. Extracts were stored at −80 °C. Analyses were performed on an Ultimate 3000 System (Dionex, LC Packings, Sunnyvale, CA) consisting of an autosampler with cooled tray and a column oven with a switching unit coupled to an LTQ Orbitrap XL (Thermo Scientific, Waltham, MA). A Phenomenex Strata X 2.0 × 20-mm cartridge (Torrance, CA) and a Waters XBridge column (2.1 × 50 mm, 2.5 μm) (Milford, MA) were used for on-line solid phase extraction and as analytical column, respectively. Positive electrospray ionization-mass spectrometry was performed by high resolution mass spectrometry (scan range 150–2000 *m*/*z*, resolution 60,000). Compound identities were confirmed

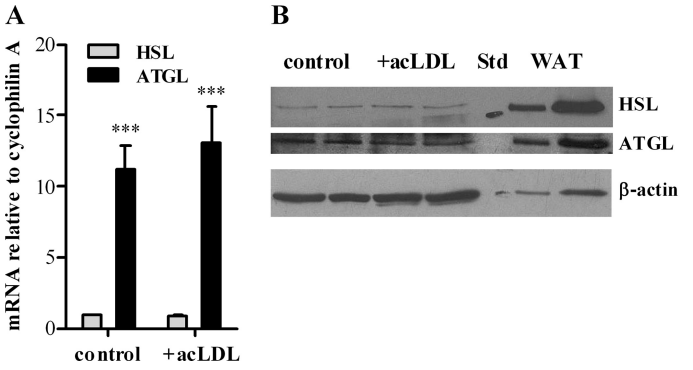

FIGURE 1. **ATGL expression in macrophages and foam cells.** Mouse peritoneal macrophages, human THP-1, and human monocyte-derived macrophages (*HMDM*) were cultivated in DMEM, 10% LPDS in the absence (control) or presence of 100 μg of acLDL/ml. Total RNA was isolated and reverse-transcribed, and mRNA expression of ATGL (*A* and *C*) and hormone-sensitive lipase (*HSL*) was determined by real time PCR, including murine hypoxanthine-guanine phosphoribosyltransferase or human (*hu*) porphobilinogen deaminase normalization (*A*). Untreated macrophages were arbitrarily set to 1. Data are expressed as mean values ($n = 3$) ± S.E. of triplicate repeats. ***, $p \leq 0.001$. *B,* cell extracts of macrophages, foam cells (40 μg per lane), and white adipose tissue (*WAT*) (10 and 40 μg per lane) were resolved by SDS-PAGE. Protein expression of ATGL and hormone-sensitive lipase were analyzed by Western blotting relative to the expression of β-actin. *STD,* standard.

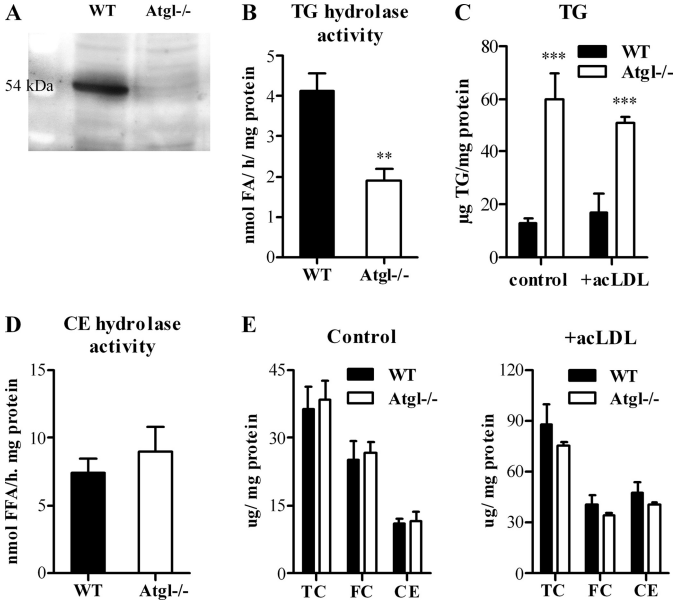

FIGURE 2. **Analysis of hydrolase activities and lipid parameters of *Atgl*$^{-/-}$ and WT macrophages.** *A,* Western blotting of WT and *Atgl*$^{-/-}$ MPM using an anti-ATGL-specific antibody. *B,* TG. *D,* CE hydrolase activities were assayed in cell lysates from WT and *Atgl*$^{-/-}$ MPM. Lipids from MPM (control) and 24-h acetylated LDL-loaded (100 μg/ml) MPM (+*acLDL*) were extracted. *C,* TG. *E,* (total cholesterol), FC, and CE concentrations were measured enzymatically. Data are presented as mean values ($n = 3$–4) ± S.E. ***, $p \leq 0.001$.

using accurate mass, tandem mass spectrometry, and retention time. Peak area ratios of acylcarnitines were compared with C17:0 CoA for semiquantitative analysis.

Phagocytosis of Fluorescein-labeled Escherichia coli Particles—MPM of *Atgl*$^{-/-}$ and WT mice were plated in black 96-well μClear plates (Greiner Bio-One GmbH, Solingen, Germany). After 24 h of preincubation in DMEM, 10% LPDS, and 25 mM glucose, cells were incubated in DMEM, 10% LPDS and 0, 6, or 25 mM glucose for 1 and 8 h, respectively. After washing the cells, 100 μl of fluorescein-labeled *E. coli* BioParticles® (Vybrant™ Phagocytosis Assay, Molecular Probes, Invitrogen) suspended in Hanks' balanced salt solution were added for 2 h. The suspension was then removed, and subsequently, 100 μl of trypan blue suspension was added for 1 min to quench the extracellular probe. After aspiration of trypan blue from experimental and control wells, the fluorescence was measured at 484 (excitation) and 535 nm (emission) on a Victor 1420 multilabel counter (PerkinElmer Life Sciences). Phagocytosis was normalized to protein content in each well. To analyze phagocytosis *in vivo*, mice were injected intraperitoneally with 200 μl of fluorescein-labeled *E. coli* BioParticles® (Molecular Probes, Invitrogen) suspended in Hanks' balanced salt solution. After 2 h, MPM were collected by flushing the peritoneal cavity with 10 ml of PBS plus 1 mM EDTA and incubated in DMEM containing 25 mM glucose and 10% LPDS for 90 min. The cells were then washed three times with PBS, and the fluorescence was measured before and after adding trypan blue suspension to obtain total and intracellular fluorescence, respectively. Experimental readings were normalized to protein content.

Phagocytosis of Yeast Cells—Yeast cells were cultured in potato dextrose broth for 48 h and autoclaved at 120 °C for 45 min. Cells were washed three times with PBS and then stored at 4 °C. Before use, the cells were sonicated for a short time and diluted to 10^8 cells/ml of DMEM. *Atgl*$^{-/-}$ and WT macrophages were plated on chamber slides and preincubated for 24 h in DMEM, 10% LPDS. Thereafter, cells were washed with PBS and incubated for 8 h in DMEM, 10% LPDS media containing 0, 6, and 25 mM glucose, respectively. After incubation, yeast cells (~10^8 cells/ml) were added and incubated for 1 h. Nonengulfed yeast cells were washed with PBS. One ml of 1% tannic acid solution was added for 1 min, and cells were then washed and air-dried. Cells were stained for 2 min with May-Grünwald stain freshly diluted with Giemsa buffer (1:2), washed with PBS, and dried. Cells were mounted in Vectashield medium plus 4′,6-diamidino-2-phenylindole (Vector Laboratories, Burlingame, CA). Visualization of the images was performed on a TissueFAXS (TissueGnostics, Vienna, Austria) assembled with an AxioImager.Z1 automated microscope (Carl Zeiss GmbH, Oberkochen, Germany). Pictures (×63) were taken at 560 nm excitation/630 nm emission (Texas Red filter), and MPM nuclei were observed at 390 nm excitation/450 nm emission (4′,6-diamidino-2-phenylindole).

Statistics—Statistical analyses in experiments, except for real time PCR analyses (see above), were performed with GraphPad Prism 5.0. The significance was determined by Student's *t* test. Data with >2 groups or ≥2 of independent variables were analyzed with one-way analysis of variance followed by the Bonferroni post hoc test. Data are presented as mean values ± S.E. *, $p < 0.05$; **, $p \leq 0.01$; ***, $p \leq 0.001$.

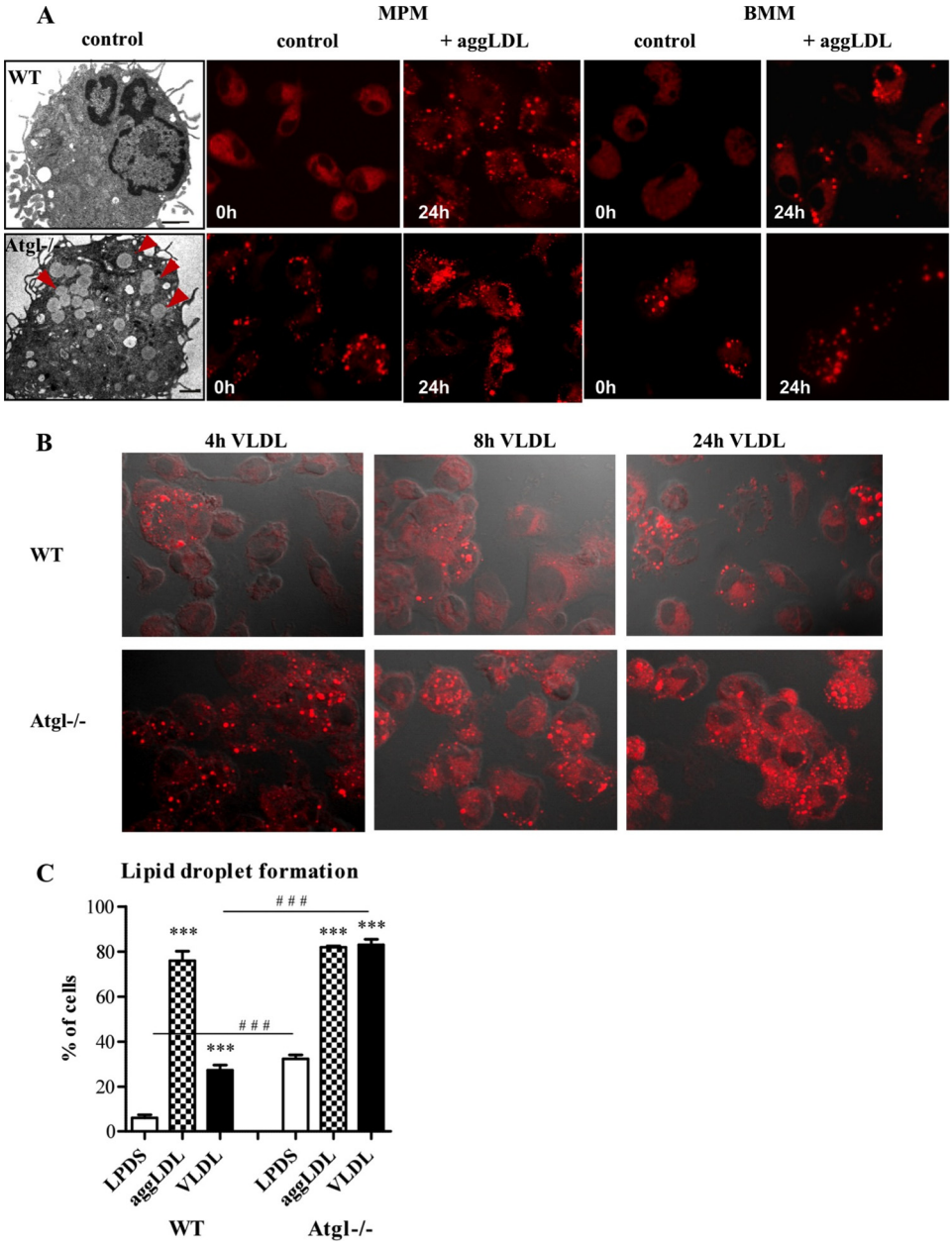

FIGURE 3. **Lipid droplets in *Atgl*$^{-/-}$ and WT macrophages.** *A*, electron microscopy images of an *Atgl*$^{-/-}$ and WT macrophage. Lipid droplets in the *Atgl*$^{-/-}$ macrophage are indicated by *arrowheads*. *A* and *B*, fluorescent microscopy images after Nile Red staining of *Atgl*$^{-/-}$ and WT MPM, BMM, and macrophages incubated with 100 μg of aggLDL/ml for 24 h (*A*) or MPM incubated with 100 μg of VLDL/ml for 4, 8 and 24 h (*B*). *Scale bar* in electron microscopy images applies to 1 μm. Fluorescence images: original magnification, ×63. *C*, quantification of lipid droplet-containing cells in MPM cultivated in LPDS or after incubation with aggLDL or VLDL for 24 h. Data are presented as the mean percent ± S.E. of foamy-like cells from at least 150 cells per group. ***, $p \leq 0.001$; ###, $p \leq 0.001$.

RESULTS

ATGL Is Expressed in Macrophages and Foam Cells—We investigated ATGL mRNA expression levels in macrophages and foam cells. Although less than in white adipose tissue, ATGL mRNA was expressed in both MPM and macrophage-derived foam cells. Foam cell formation was achieved after loading MPM with acLDL. ATGL mRNA levels in macrophages and foam cells were 11.2- and 15.5-fold increased compared with hormone-sensitive lipase mRNA (Fig. 1*A*). In accordance with mRNA levels, ATGL protein expression was comparable in macrophages and foam cells but markedly lower than in white adipose tissue. Concomitantly, we found less hormone-sensitive lipase protein in macrophages and foam cells compared with ATGL (Fig. 1*B*). ATGL mRNA was also significantly expressed in human monocyte-derived macrophages and foam cells (Fig. 1*C*). Human ATGL mRNA expression was markedly higher in primary cells than in THP1-derived macrophages and foam cells.

Reduced TG Hydrolase Activity and Increased TG Content in Atgl$^{-/-}$ *Macrophages*—TG hydrolase activity was determined in MPM isolated from WT and *Atgl*$^{-/-}$ mice. We verified the lack of ATGL in macrophages by Western blotting (Fig. 2*A*). TG hydrolase activity was significantly (−54%) decreased in *Atgl*$^{-/-}$ compared with WT MPM (Fig. 2*B*). Concomitantly, *Atgl*$^{-/-}$ MPM showed higher TG concentrations in MPM and acLDL-loaded foam cells (4.7- and 3.0-fold, respectively) (Fig. 2*C*). In contrast, MPM of *Atgl*$^{-/-}$ and WT mice exhibited comparable CE hydrolase activities (Fig. 2*D*). Accordingly, intracellular total cholesterol, FC, and CE concentrations in MPM and foam cells of both genotypes were similar (Fig. 2*E*).

Increased Lipid Droplet Numbers in Atgl$^{-/-}$ *Macrophages*—Lipid droplets were visualized by electron microscopy in *Atgl*$^{-/-}$ and WT MPM and by fluorescence microscopy of Nile Red-stained WT and *Atgl*$^{-/-}$ MPM as well as in bone marrow-derived macrophages (BMM) (Fig. 3). In MPM and BMM isolated from WT mice, only a few lipid droplets were visible, whereas in *Atgl*$^{-/-}$ MPM the number of lipid droplets markedly increased (Fig. 3*A*). After cultivation in medium containing aggregated (agg)LDL for 24 h, MPM and BMM of both genotypes accumulated lipids in comparable amounts (Fig. 3*A*). Similar results were obtained after incubation of MPM with acLDL for 24 h (data not shown). Incubation of MPM with VLDL for 4, 8, and 24 h resulted in increased lipid droplet formation in *Atgl*$^{-/-}$ compared with WT cells (Fig. 3*B*). Quantification of lipid droplet-containing WT and *Atgl*$^{-/-}$ MPM incubated in the absence or presence of aggLDL or VLDL is shown in Fig. 3*C*. The data reveal that MPM cultured in

medium containing lipoprotein-deficient serum (LPDS) had 5.4-fold more Nile Red-stained neutral lipids compared with WT MPM (Fig. 3*C*). After incubation with aggLDL for 24 h, MPM of WT and *Atgl*$^{-/-}$ mice showed the same amount of lipid droplet-containing cells. VLDL loading, however, led to a 3.0-fold increase in lipid droplet accumulation in *Atgl*$^{-/-}$ compared with WT macrophages (Fig. 3*C*). This difference was due to the fact that *Atgl*$^{-/-}$ MPM already had 5.4-fold more foamy cells compared with WT macrophages in the absence of exogenous lipids.

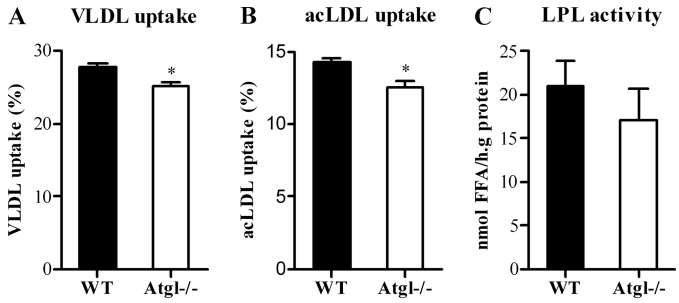

FIGURE 4. **Lipoprotein uptake and LPL activity in *Atgl*$^{-/-}$ and WT macrophages.** MPM from WT and *Atgl*$^{-/-}$ mice were incubated with [^{3}H]VLDL (*A*) or [^{3}H]acLDL (*B*) for 24 h. VLDL and acLDL uptake in *Atgl*$^{-/-}$ and WT MPM was assessed by liquid scintillation. *C,* WT and *Atgl*$^{-/-}$ MPM were incubated with [^{3}H]triolein for 1 h and assayed for LPL activity. Data are presented as mean values ($n = 3$–5) performed in duplicate ± S.E. *, $p < 0.05$.

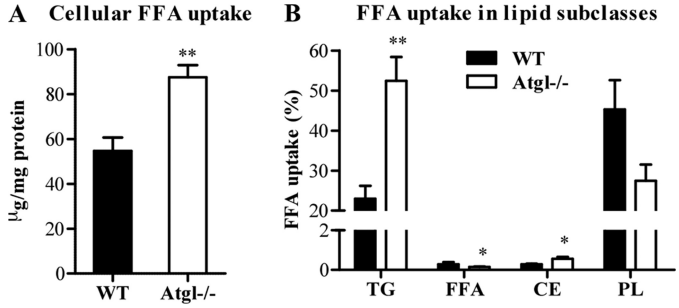

FIGURE 5. **FFA uptake in *Atgl*$^{-/-}$ and WT macrophages.** MPM from *Atgl*$^{-/-}$ and WT mice were incubated with [^{3}H]oleate for 24 h. Lipids were extracted, and lipid subclasses were separated by TLC. The uptake of oleate in whole cells (*A*) and various lipid subclasses (*B*) was determined by liquid scintillation counting. Data are presented as mean values ($n = 3$–4) performed in triplicate ± S.E. *, $p < 0.05$; **, $p \leq 0.01$. *PL*, phospholipid.

To determine whether WT and *Atgl*$^{-/-}$ macrophages show differences in lipoprotein uptake, cells were incubated with [^{3}H]TG-labeled VLDL or [^{3}H]cholesterol-labeled acLDL. The uptake of both lipoproteins was marginally but significantly decreased ($p < 0.05$) in *Atgl*$^{-/-}$ *versus* WT cells (Fig. 4, *A* and *B*). Since LPL is responsible for the extracellular hydrolysis of lipoprotein-associated TG and the subsequent uptake of FFAs in underlying cells and tissues, we determined LPL activity in *Atgl*$^{-/-}$ and WT MPM. LPL activity was unchanged in *Atgl*$^{-/-}$ compared with WT MPM (Fig. 4*C*).

Increased FFA Uptake by Atgl$^{-/-}$ *Macrophages*—FFA uptake was examined in *Atgl*$^{-/-}$ and WT MPM after incubation with [^{3}H]oleate for 24 h. We observed a 1.6-fold increase in oleate uptake in *Atgl*$^{-/-}$ compared with WT MPM (Fig. 5*A*). We used TLC to analyze the incorporation of radioactivity into lipid subclasses of *Atgl*$^{-/-}$ and WT MPM. ATGL deficiency in MPM resulted in increased incorporation of radiolabeled oleate in the TG and CE fractions (2.3- and 2.0-fold, respectively) (Fig. 5*B*). The incorporation of oleate into PL was slightly reduced, but the difference did not reach statistical significance. The concentration of FFAs in WT MPM was very low compared with TG, and it was even lower in *Atgl*$^{-/-}$ MPM.

Reduced ATP Concentration and Increased ADP/ATP Ratios in Atgl$^{-/-}$ *Macrophages*—FAs are an important oxidative fuel in many mammalian cell types. To determine whether the lower cellular FA concentration in *Atgl*$^{-/-}$ MPM had an impact on energy production, we measured ATP concentrations in *Atgl*$^{-/-}$ and WT MPM cultured for 24 h in media with different glucose concentrations (0, 6, and 25 mM). Oligomycin, an inhibitor of mitochondrial F_1F_0-ATP synthase, was used as an ATP-depletion control for the assay. Oligomycin completely blocked the energy production in WT and *Atgl*$^{-/-}$ MPM. Importantly, the ATP level was substantially decreased (−65%) in *Atgl*$^{-/-}$ MPM compared with WT MPM in the absence of glucose (Fig. 6*A*). Significant reductions, although less pronounced, were observed even in media containing 6 or 25 mM glucose (−22 and −27%, respectively). Next, we determined ADP/ATP ratios since the total amount of the sum of ATP + ADP is expected to remain fairly constant. In all cultivation conditions, the ADP/ATP ratios were markedly increased in *Atgl*$^{-/-}$ compared with WT MPM (Fig. 6*B*). In glucose-free medium, the ADP/ATP ratio was substantially elevated also in WT macrophages compared with glucose-containing medium, indicating reduced cell vitality. In *Atgl*$^{-/-}$ MPM, this increase was even more pronounced.

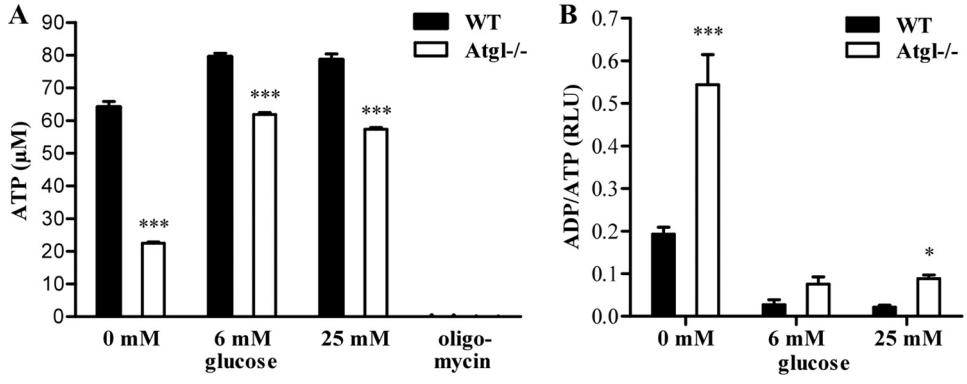

FIGURE 6. **ATP concentrations and ADP/ATP ratios in *Atgl*$^{-/-}$ and WT macrophages.** *A*, ATP levels in *Atgl*$^{-/-}$ and WT MPM were measured after cultivating the cells for 24 h in DMEM, 10% LPDS containing 0, 6, and 25 mM glucose. Oligomycin (0.5 µM) was used as an ATP-depletion control. Data are presented as mean values ($n = 4$) ± S.E. ***, $p \leq 0.001$. *B,* ADP/ATP ratios in *Atgl*$^{-/-}$ and WT MPM were determined using the EnzyLight™ ADP/ATP ratio assay kit. Data are expressed as mean values ($n = 4$) ± S.E. *, $p < 0.05$; ***, $p \leq 0.001$.

Impaired Phagocytosis Ability in Atgl$^{-/-}$ *Macrophages*—Phagocytosis is a highly energy demanding process. Therefore, we hypothesized that the decreased FA availability and ATP concentration in *Atgl*$^{-/-}$ MPM may impact their phagocytotic capacity. To test this hypothesis, *Atgl*$^{-/-}$ and WT MPM were cultured in media containing

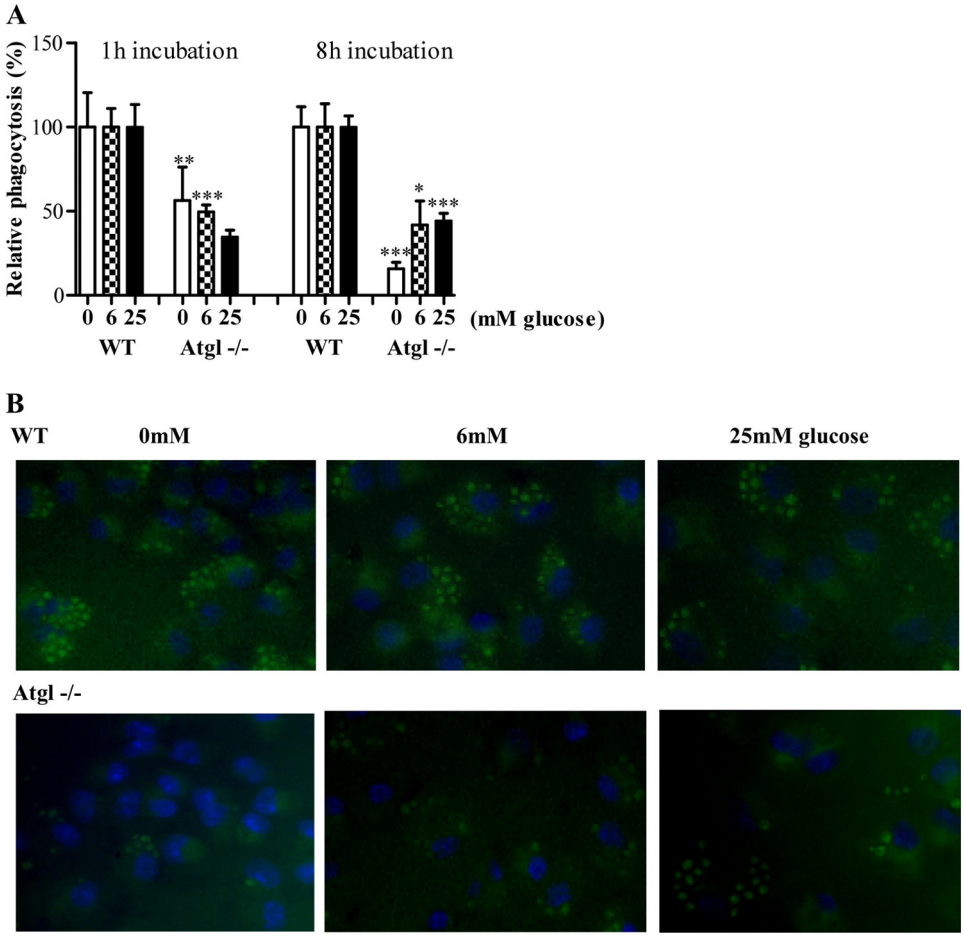

FIGURE 7. **Phagocytosis in *Atgl*$^{-/-}$ and WT macrophages.** *A,* MPM from *Atgl*$^{-/-}$ and WT mice were cultivated in DMEM, 10% LPDS with 0, 6, and 25 mM glucose for 1 and 8 h, respectively. Phagocytosis of fluorescein-labeled *E. coli* particles is presented as mean values ($n = 6$) ± S.E. of two independent experiments. Phagocytosis of WT cells was arbitrarily set to 100%. *, $p < 0.05$; **, $p \leq 0.01$; ***, $p \leq 0.001$. *B,* representative images showing phagocytosis of yeast cells by *Atgl*$^{-/-}$ and WT MPM after 8 h of cultivation in DMEM, 10% LPDS containing 0, 6, and 25 mM glucose. Original magnification, ×63.

0, 6, and 25 mM glucose for 1 and 8 h, respectively. Independent of the presence or absence of glucose, we observed a decreased ability of *Atgl*$^{-/-}$ MPM to engulf fluorescein-labeled *E. coli* particles compared with WT cells (Fig. 7*A*). These differences were more pronounced after 8 h of incubation, especially under glucose-free conditions. Phagocytosis was markedly reduced in the absence of glucose (−84%). Even in the presence of 6 and 25 mM glucose, the phagocytotic capacity was significantly reduced (−58 and −56%, respectively) (Fig. 7*A*).

To support our findings, we performed the experiment using yeast cells as particles to be phagocytosed by MPM. *Atgl*$^{-/-}$ MPM cultivated for 8 h in glucose-free medium almost lacked phagocytotic properties (Fig. 7*B*). The increase of glucose concentrations in the medium concomitantly increased the ability of *Atgl*$^{-/-}$ cells to phagocytose yeast. In contrast, WT macrophages showed similar capacities to engulf yeast independent of glucose concentrations. In addition, we checked phagocytosis in *Atgl*$^{-/-}$ mice *in vivo*. Although total fluorescence was less in macrophages isolated from *Atgl*$^{-/-}$ mice 2 h after injection of fluorescent *E. coli* particles, this decrease did not reach significance (Fig. 8*A*). However, after quenching external fluorescence of *E. coli* particles, which have not been internalized by the macrophages and therefore stained by trypan blue, phagocytosis was significantly reduced in *Atgl*$^{-/-}$ mice (Fig. 8*B*). Internalization was also visualized by fluorescence microscopy (Fig. 8*C*).

Reduced Expression of Mitochondrial Genes and Acylcarnitines in Atgl$^{-/-}$ *Macrophages*—Efficient FA oxidation and ATP synthesis not only depend on substrate availability but also on effective FA transport into the mitochondria and on mitochondrial function. To elucidate whether a decreased oxidative capacity contributes to the reduced phagocytotic capacity of *Atgl*$^{-/-}$ macrophages, we analyzed the expression of carnitine palmitoyltransferase 1a and long chain acyl-CoA dehydrogenase, two important proteins in mitochondrial fatty acid β-oxidation. mRNA levels of both genes were markedly decreased in *Atgl*$^{-/-}$ MPM (−58 and −63%, respectively), and foam cells (−58 and −57%, respectively) (Fig. 9, *A* and *B*). Total acyl-CoA concentrations were decreased by 31% in *Atgl*$^{-/-}$ compared with MPM (Fig. 9*C*). The most significant reduction was observed in acetyl-CoA levels. Long chain acyl-CoAs showing a trend toward decreased levels in *Atgl*$^{-/-}$ macrophages, however, failed to reach statistical significance. Finally, we found 39% reduced total carnitine ester levels in *Atgl*$^{-/-}$ compared with WT MPM (Fig. 9*D*). Essentially all middle and long chain carnitine esters were decreased with significant reductions in 12:1, 14.0, 14:1, and 16:1 carnitine esters.

DISCUSSION

Previous studies have demonstrated that ATGL is the rate-limiting enzyme for the hydrolysis of intracellular TG in adipose and many nonadipose tissues of mice and humans (22–25, 37). ATGL deficiency in mice causes TG accumulation in essentially all tissues. Lipid deposition is mostly pronounced in cardiac and skeletal muscle, testis, kidney, and pancreas (25). Massive lipid accumulation in cardiac myocytes causes cardiac failure and premature death of *Atgl*$^{-/-}$ mice starting at the age of 10 weeks. Due to the reduced availability of FAs as energy substrate, *Atgl*$^{-/-}$ mice show an increased utilization of carbohydrates as an energy source, leading to improved glucose tolerance and insulin sensitivity (25). We hypothesized that ATGL is also involved in macrophage TG catabolism providing FAs as oxidative substrate for energy synthesis. This process might be

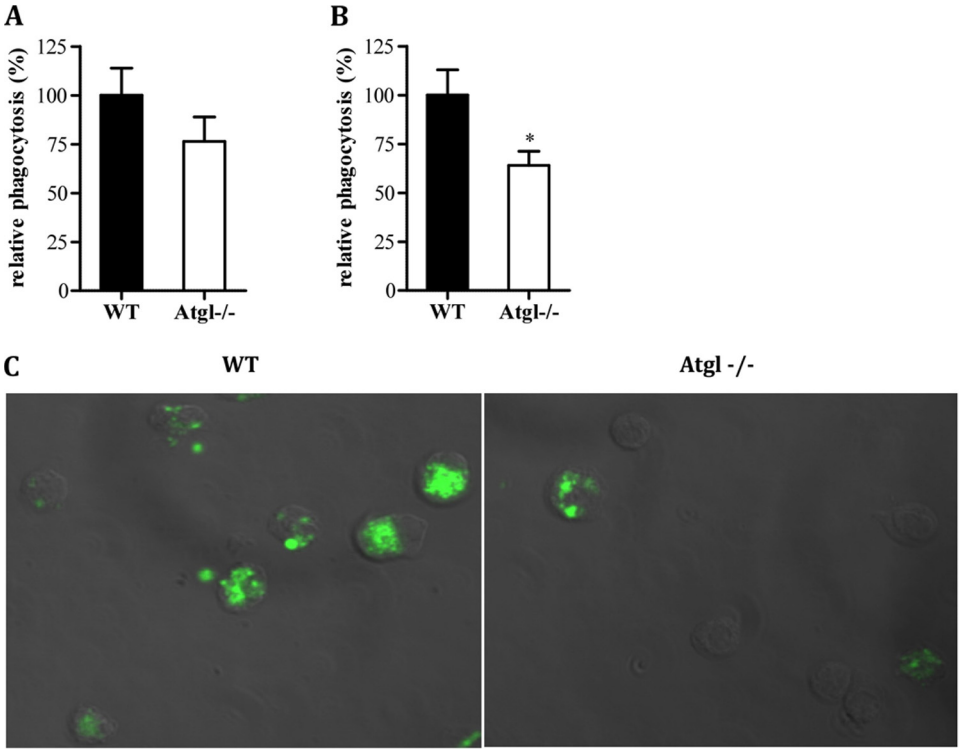

FIGURE 8. **Phagocytosis in *Atgl*$^{-/-}$ and WT mice *in vivo*.** Fluorescein-labeled *E. coli* particles (200 μl) were injected into *Atgl*$^{-/-}$ and WT mice. After 2 h, peritoneum was flushed with 10 ml of PBS, 1 mM EDTA, and macrophages were isolated and assayed for total (*A*) and internalized (*B*) fluorescence after quenching of extracellular fluorescence by trypan blue. *C,* representative image showing total fluorescence in WT and *Atgl*$^{-/-}$ MPM. Original magnification, ×63. Phagocytosis of WT cells was arbitrarily set to 100%. Relative phagocytosis is presented as mean values ($n = 8–9$) ± S.E. of three independent experiments. *, $p < 0.05$.

very important with respect to energy-consuming phagocytosis and consequently the immune host defense.

Compared with the hormone-sensitive lipase, an enzyme implicated in TG and CE hydrolysis in many tissues and in macrophages, ATGL is highly expressed in mouse macrophages and foam cells. Absence of ATGL in macrophages leads to significantly decreased TG hydrolase activity and, concomitantly, increased intracellular TG concentrations. In contrast, and in accordance with the substrate specificity of ATGL, CE hydrolase activity is similar in *Atgl*$^{-/-}$ and WT macrophages. Even in the absence of exogenous lipid loading *Atgl*$^{-/-}$, macrophages accumulate TG demonstrating the critical role of ATGL in macrophage TG catabolism. In atherosclerotic lesions, macrophage-derived foam cells have a large number of lipid droplets filled with CE, which can be hydrolyzed to FC and FFAs by the action of a neutral CE hydrolase. In contrast to WT foam cells, *Atgl*$^{-/-}$ macrophages accumulate specifically TG, whereas CE and FC concentrations are unchanged compared with control cells. This allowed us to study the direct effects of defective TG hydrolysis on macrophage function without the accompanying impact of ATGL on cellular cholesterol catabolism.

We hypothesized that the decreased availability of FFAs generated by the hydrolysis of cellular TG stores may be compensated by an increased uptake of extracellular FFAs mediated by LPL-dependent and -independent mechanisms. However, the absence of macrophage ATGL did not result in major differences in acLDL or VLDL uptake or in LPL activity. These data implicate that FAs generated by the action of LPL are taken up similarly by *Atgl*$^{-/-}$ and WT macrophages. As a compensatory mechanism, the uptake of exogenously added FFAs was increased in *Atgl*$^{-/-}$ macrophages. However, this elevated uptake failed to normalize cellular FFA levels. This finding implies that the majority of FFAs taken up by *Atgl*$^{-/-}$ macrophages is re-esterified and neutralized within TG, probably preventing the potential cytotoxic effect of increasing amounts of intracellular FFA levels. Our data strongly suggest that FAs taken up by *Atgl*$^{-/-}$ (and WT) macrophages are not directly routed to mitochondrial β-oxidation but first have to be esterified to TG (and CE) for the subsequent usage as energy substrate generated by ATGL hydrolysis (and probably the activity of neutral CE hydrolases).

In many tissues, TG play a major role in supplying FAs as energy substrate. In addition, TG serve as an important storage pool for FFAs that are used for the synthesis of phospholipids, ceramides, and other complex lipids. Glucose has been proposed to be the major energy substrate in macrophages (6, 7). FAs are used as alternative energy fuel taken up by lipoprotein-mediated TG catabolism or whole lipoprotein particle uptake. After cultivating macrophages for 24 h in media containing different concentrations of glucose, we found that ATP levels were markedly reduced in the absence of ATGL, whereas ADP/ATP ratios increased. Our findings clearly show that macrophages store TG and use this TG pool as energy substrate even in the presence of glucose. This pathway can be particularly important under starving conditions or in conditions of decreased glucose usage like in the diabetic state.

To address the impact of reduced FFA availability and consequently decreased ATP generation, we investigated the *in vitro* and *in vivo* phagocytotic capacity of *Atgl*$^{-/-}$ macrophages. Importantly, phagocytosis was decreased in *Atgl*$^{-/-}$ mice. Moreover, the phagocytotic capacity was affected by the lack of ATGL even in the presence of glucose *in vitro*, albeit to a lesser extent than in glucose-free medium. This finding parallels our data on intracellular energy stores, which are also decreased in *Atgl*$^{-/-}$ MPM when cultivated in glucose-containing media. Yin *et al.* (3) found that LPL-mediated FA release provided energy for macrophages under conditions of limited amounts of ambient glucose and during periods of intense metabolic activity, such as phagocytosis. Since reduced phagocytosis was not observed in glucose-containing medium, the authors suggested that macrophages do not endocytose sufficient lipoproteins from the medium and/or hydrolyze sufficient lipoproteins

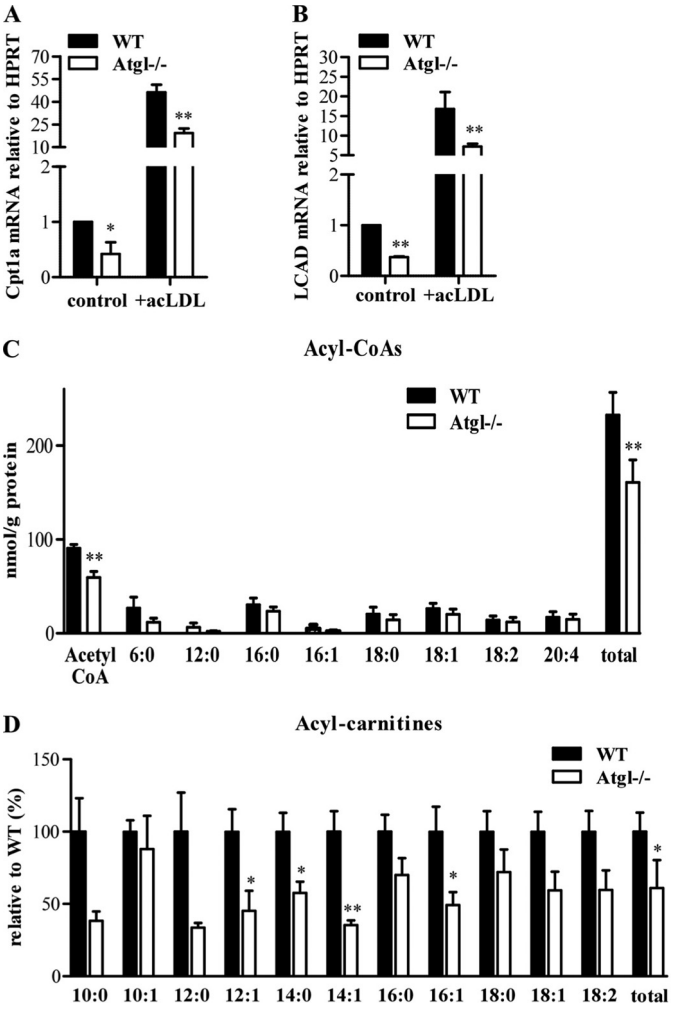

FIGURE 9. **mRNA levels of mitochondrial genes in *Atgl*$^{-/-}$ and WT macrophages and foam cells.** MPM were cultivated in DMEM, 10% LPDS in the absence or presence of 100 μg of acLDL/ml (foam cells). Total RNA was isolated from cells and reverse-transcribed, and mRNA levels of carnitine palmitoyltransferase (*CPT*)1a (*A*) and long chain acyl-CoA dehydrogenase (*LCAD*) (*B*) were determined by real time PCR, including normalization to hypoxanthine-guanine phosphoribosyltransferase (*HPRT*) levels. Untreated MPM were arbitrarily set to 1. Data are expressed as mean values ± S.E. of triplicate repeats. *C,* long chain acyl-CoA. *D,* carnitine ester concentrations were determined in macrophages of *Atgl*$^{-/-}$ and WT mice. Data are expressed as mean values ($n = 4–5$) ± S.E. correlated to protein concentrations. *, $p < 0.05$; **, $p \leq 0.01$.

intracellularly to provide comparable amounts of FAs for phagocytosis (3). We propose that ATGL plays an essential role in meeting the high energy demand of macrophages during phagocytosis. However, in contrast to extracellular LPL-mediated FA mobilization, intracellular ATGL-mediated FFA release is essential for maximal phagocytotic activity even when glucose is available. We hypothesize that this finding is the consequence of different utilization of particular FA pools inside the cell. (i) FAs taken up by macrophages from outside the cell are not directly available as substrate for subsequent utilization, because they are esterified and stored in TG. (ii) FAs released from intracellular TG-hydrolysis by ATGL are carried into the mitochondria and used for mitochondrial FA β-oxidation and subsequent energy production. Although long chain acyl-CoA concentrations were unaffected in *Atgl*$^{-/-}$ MPM, reduced Cpt1a mRNA results in a decreased amount of carnitine esters. Unchanged steady-state concentrations of acyl-CoAs might be the consequence of reduced FFA concentrations as substrates and reduced carnitine esters as products. Decreased concentrations of acetyl-CoA confirmed defective β-oxidation and indicated that less NADH and $FADH_2$ are available for oxidative phosphorylation to drive ATP synthesis.

Our data support a critical role of TG-mediated supply of FAs as energy substrates for ATP synthesis necessary for phagocytosis. We conclude that the lipolytic defect affects the usage of FAs as energy fuel. Efficient FA oxidation and ATP synthesis not only depend on substrate availability but also on effective FA transport into the mitochondria and on mitochondrial function. In addition to FFAs as peroxisome proliferator-activated receptor signaling molecules, the homeostasis of intracellular signaling lipids involved in vesicular trafficking and phagocytosis (such as phosphatidic acid and diacylglycerol) is likely affected in *Atgl*$^{-/-}$ macrophages. Moreover, the accumulation of lipid droplets themselves may additionally account for the observed reduction in phagocytosis even in conditions in which ATP concentrations are partly restored by glucose in the medium.

In normal physiology, macrophage phagocytosis plays an essential role on host defense through clearance of infectious organisms and in the resolution phase of inflammation, through clearance of apoptotic cells (efferocytosis) and inflammatory debris (38). In atherogenesis, macrophage phagocytosis can either promote or protect against lesion progression, depending on the context (39–41). On the one hand, the phagocytic uptake of aggregated lipoproteins can promote foam cell formation and atherogenesis (40). Phagocytosis of erythrocytes and platelets may also promote lesion progression (40). If this hypothesis is true, deficiency of ATGL in macrophages might result in reduced atherosclerosis susceptibility. On the other hand, efferocytosis of apoptotic cells in lesions reduces plaque progression by decreasing lesion cellularity, preventing post-apoptotic necrosis, and promoting anti-inflammatory response (42). Future *in vivo* studies exploring the possible roles of macrophage ATGL in host defense, inflammation resolution, and atherosclerosis should be addressable using the mouse models and concepts described in this study.

Acknowledgments—We thank S. Povoden, E. Stanzer, A. Ibovnik, T. Kueznik, and M. Absenger for excellent technical assistance and A. Hermann and I. Hindler for caring for the mice used in this study.

REFERENCES

1. Speert, D. P., and Gordon, S. (1992) *J. Clin. Invest.* **90,** 1085–1092
2. Simon, L. M., Axline, S. G., Horn, B. R., and Robin, E. D. (1973) *J. Exp. Med.* **138,** 1413–1425
3. Yin, B., Loike, J. D., Kako, Y., Weinstock, P. H., Breslow, J. L., Silverstein, S. C., and Goldberg, I. J. (1997) *J. Clin. Invest.* **100,** 649–657
4. Bates, S. R., Murphy, P. L., Feng, Z. C., Kanazawa, T., and Getz, G. S. (1984) *Arteriosclerosis* **4,** 103–114
5. Huff, M. W., Evans, A. J., Sawyez, C. G., Wolfe, B. M., and Nestel, P. J. (1991) *Arterioscler. Thromb.* **11,** 221–233
6. Jong, M. C., Hendriks, W. L., van Vark, L. C., Dahlmans, V. E., Groener, J. E., and Havekes, L. M. (2000) *Arterioscler. Thromb. Vasc. Biol.* **20,** 144–151
7. Lindqvist, P., Ostlund-Lindqvist, A. M., Witztum, J. L., Steinberg, D., and

Little, J. A. (1983) *J. Biol. Chem.* **258,** 9086–9092
8. Renier, G., Skamene, E., DeSanctis, J. B., and Radzioch, D. (1993) *Arterioscler. Thromb.* **13,** 190–196
9. Babaev, V. R., Fazio, S., Gleaves, L. A., Carter, K. J., Semenkovich, C. F., and Linton, M. F. (1999) *J. Clin. Invest.* **103,** 1697–1705
10. Babaev, V. R., Patel, M. B., Semenkovich, C. F., Fazio, S., and Linton, M. F. (2000) *J. Biol. Chem.* **275,** 26293–26299
11. Van Eck, M., Zimmermann, R., Groot, P. H., Zechner, R., and Van Berkel, T. J. (2000) *Arterioscler. Thromb. Vasc. Biol.* **20,** E53–E62
12. Brasaemle, D. L. (2007) *J. Lipid Res.* **48,** 2547–2559
13. Londos, C., Brasaemle, D. L., Schultz, C. J., Segrest, J. P., and Kimmel, A. R. (1999) *Semin. Cell Dev. Biol.* **10,** 51–58
14. Martin, S., and Parton, R. G. (2006) *Nat. Rev. Mol. Cell Biol.* **7,** 373–378
15. Kruth, H. S., Jones, N. L., Huang, W., Zhao, B., Ishii, I., Chang, J., Combs, C. A., Malide, D., and Zhang, W. Y. (2005) *J. Biol. Chem.* **280,** 2352–2360
16. Xu, X. X., and Tabas, I. (1991) *J. Biol. Chem.* **266,** 24849–24858
17. Unger, R. H., and Orci, L. (2002) *Biochim. Biophys. Acta* **1585,** 202–212
18. Brown, M. S., Ho, Y. K., and Goldstein, J. L. (1980) *J. Biol. Chem.* **255,** 9344–9352
19. Tabas, I. (2002) *J. Clin. Invest.* **110,** 905–911
20. Warner, G. J., Stoudt, G., Bamberger, M., Johnson, W. J., and Rothblat, G. H. (1995) *J. Biol. Chem.* **270,** 5772–5778
21. Feng, B., Yao, P. M., Li, Y., Devlin, C. M., Zhang, D., Harding, H. P., Sweeney, M., Rong, J. X., Kuriakose, G., Fisher, E. A., Marks, A. R., Ron, D., and Tabas, I. (2003) *Nat. Cell Biol.* **5,** 781–792
22. Zimmermann, R., Strauss, J. G., Haemmerle, G., Schoiswohl, G., Birner-Gruenberger, R., Riederer, M., Lass, A., Neuberger, G., Eisenhaber, F., Hermetter, A., and Zechner, R. (2004) *Science* **306,** 1383–1386
23. Jenkins, C. M., Mancuso, D. J., Yan, W., Sims, H. F., Gibson, B., and Gross, R. W. (2004) *J. Biol. Chem.* **279,** 48968–48975
24. Villena, J. A., Roy, S., Sarkadi-Nagy, E., Kim, K. H., and Sul, H. S. (2004) *J. Biol. Chem.* **279,** 47066–47075
25. Haemmerle, G., Lass, A., Zimmermann, R., Gorkiewicz, G., Meyer, C., Rozman, J., Heldmaier, G., Maier, R., Theussl, C., Eder, S., Kratky, D., Wagner, E. F., Klingenspor, M., Hoefler, G., and Zechner, R. (2006) *Science* **312,** 734–737
26. Haemmerle, G., Zimmermann, R., Hayn, M., Theussl, C., Waeg, G., Wagner, E., Sattler, W., Magin, T. M., Wagner, E. F., and Zechner, R. (2002) *J. Biol. Chem.* **277,** 4806–4815
27. Escary, J. L., Choy, H. A., Reue, K., Wang, X. P., Castellani, L. W., Glass, C. K., Lusis, A. J., and Schotz, M. C. (1999) *J. Lipid Res.* **40,** 397–404
28. Osuga, J., Ishibashi, S., Oka, T., Yagyu, H., Tozawa, R., Fujimoto, A., Shionoiri, F., Yahagi, N., Kraemer, F. B., Tsutsumi, O., and Yamada, N. (2000) *Proc. Natl. Acad. Sci. U.S.A.* **97,** 787–792
29. Contreras, J. A. (2002) *Biochem. Biophys. Res. Commun.* **292,** 900–903
30. Sekiya, M., Osuga, J., Nagashima, S., Ohshiro, T., Igarashi, M., Okazaki, H., Takahashi, M., Tazoe, F., Wada, T., Ohta, K., Takanashi, M., Kumagai, M., Nishi, M., Takase, S., Yahagi, N., Yagyu, H., Ohashi, K., Nagai, R., Kadowaki, T., Furukawa, Y., and Ishibashi, S. (2009) *Cell Metab.* **10,** 219–228
31. Fredrikson, G., Tornqvist, H., and Belfrage, P. (1986) *Biochim. Biophys. Acta* **876,** 288–293
32. Basu, S. K., Goldstein, J. L., Anderson, G. W., and Brown, M. S. (1976) *Proc. Natl. Acad. Sci. U.S.A.* **73,** 3178–3182
33. Holm, C., and Osterlund, T. (1999) in *Lipase and Phospholipase Protocols* (Doolittle, M. H., and Reue, K., eds) Vol. 109, pp. 109–121, Humana Press Inc., Totowa, NJ
34. Galluhn, D., and Langer, T. (2004) *J. Biol. Chem.* **279,** 38338–38345
35. Monick, M. M., Powers, L. S., Barrett, C. W., Hinde, S., Ashare, A., Groskreutz, D. J., Nyunoya, T., Coleman, M., Spitz, D. R., and Hunninghake, G. W. (2008) *J. Immunol.* **180,** 7485–7496
36. Magnes, C., Suppan, M., Pieber, T. R., Moustafa, T., Trauner, M., Haemmerle, G., and Sinner, F. M. (2008) *Anal Chem.* **80,** 5736–5742
37. Bezaire, V., Mairal, A., Ribet, C., Lefort, C., Girousse, A., Jocken, J., Laurencikiene, J., Anesia, R., Rodriguez, A. M., Ryden, M., Stenson, B. M., Dani, C., Ailhaud, G., Arner, P., and Langin, D. (2009) *J. Biol. Chem.* **284,** 18282–18291
38. Aderem, A., and Underhill, D. M. (1999) *Annu. Rev. Immunol.* **17,** 593–623
39. Tabas, I. (2007) *Curr. Drug Targets* **8,** 1288–1296
40. Schrijvers, D. M., De Meyer, G. R., Herman, A. G., and Martinet, W. (2007) *Cardiovasc. Res.* **73,** 470–480
41. Thorp, E., Cui, D., Schrijvers, D. M., Kuriakose, G., and Tabas, I. (2008) *Arterioscler. Thromb. Vasc. Biol.* **28,** 1421–1428
42. Tabas, I. (2005) *Arterioscler. Thromb. Vasc. Biol.* **25,** 2255–2264